Hindawi
Journal of Chemistry
Volume 2021, Article ID 9535644, 11 pages
https://doi.org/10.1155/2021/9535644

Research Article

Removal of Congo Red by Silver Carp (*Hypophthalmichthys molitrix*) Fish Bone Powder: Kinetics, Equilibrium, and Thermodynamic Study

Shahanaz Parvin, Md. Manjur Hussain, Farhana Akter, and Biplob Kumar Biswas

Department of Chemical Engineering, Jashore University of Science and Technology, Jashore 7408, Bangladesh

Correspondence should be addressed to Biplob Kumar Biswas; bk.biswas@just.edu.bd

Received 1 July 2021; Accepted 30 August 2021; Published 7 September 2021

Academic Editor: Ibrahim H. Alsohaimi

Powdered form of bones of silver carp fish, an available species in Bangladesh, was investigated as a prominent bioadsorbent for the removal of Congo red from synthetic solution. Experiments were conducted in batch process, and a number of influencing parameters, such as solution pH, adsorbent dosage, contact time, and initial Congo red concentration, were thoroughly investigated for optimization. Kinetic and equilibrium data were well described by pseudo-second-order model and Langmuir isotherm, respectively. Suitability of pseudo-second-order model to best fit with the adsorption process was corroborated by squared sum of errors analysis. Mass transfer mechanism was confirmed by intraparticle pore diffusion and Bangham's diffusion models. Maximum sorption capacity of fish bone powder was found to be 666.67 $mg{\cdot}g^{-1}$. The optimum condition (adsorbent dose: 5 $g{\cdot}L^{-1}$; pH: 2.0; operating time: 4 h) for maximum sorption was determined as well. The increasing negative value of Gibbs free energy (ΔG) with temperature rise indicated spontaneous nature and feasibility of adsorption. The positive values of ΔH and ΔS suggested that the adsorption reaction is endothermic and random (at the solid/liquid interface) in nature. The activation energy (29.84 $kJ{\cdot}mol^{-1}$) indicated that the sorption process was of physisorption type. A considerably high adsorption capacity pointed towards utilization of this apparently useless biomaterial as an effective adsorbent.

1. Introduction

Industries, such as textile, leather, pulp and paper, cotton, paint, plastic, and cosmetics, use dyes to color their products and thus consume substantially a large volume of synthetic dye as well as process water for their production. As a result, they produce a considerable amount of colored wastewater. The textile industry consumes more than ten thousand tonnes of dye per annum out of which approximately one hundred tonnes of dye are discharged annually into the water stream [1]. Although dye-containing effluent contains aesthetic contaminants, it has negative impact on overall aquatic inhabitants through reduction in phytoplankton photosynthesis [2, 3]. Toxicity, contamination by color, nonbiodegradability, and complex structure of dye can cause enormous threat to human health and the aquatic environment as a whole [4]. Several classes of dyes are reported in the literature that include anionic dyes (e.g., all sort of direct dye, acid dye, and reactive dye), cationic dyes (all basic dyes), and nonionic dye (e.g., dispersed dyes) [5].

Congo red (CR) is known to be an anionic benzidine-based diazo synthetic dye, which is characterized by large molecular structure with two azo groups that are bound to aromatic rings having recalcitrant molecular structure [6]. The effluent from the above-mentioned industries, if not treated properly, can cause severe damage to aquatic habitants. Moreover, Congo red is responsible for causing cancer to mammals. However, it is a challenging task to biodegrade Congo red due to the stability of its structure [1]. Hence, effective removal of this dye form wastewaters has to be performed before discharging into the water bodies.

Removal of dyes from water and wastewater can be done by means of any of the methods, namely, biological, chemical, and physical methods. Several wastewater

treatment techniques have been reported to treat dyes from wastewaters, which include but not limited to, biological degradation [7], membrane separation [8], electrolysis [9], and oxidation [10]. These methods are having limitations such as high cost of plant, higher operational costs, interference by another constituents, and excessive sludge generation. Adsorption, on the other hand, is a much better process for contaminants removal from wastewater because of the availability of adsorbents, efficiency of the process, uncomplicated operation, and low-cost of the adsorbent. Some conventional adsorbents were used for treating the dye-containing wastewater that includes ash, nanomaterials, and activated carbon. Nowadays biomaterials and agricultural waste materials (such as pine bark, orange peel, peanut shell, sawdust, and sunflower) are getting more priority from the researchers throughout the world [11–13]. In this context, adsorption of CR by using waste biomaterials would have been a promising process in the field of wastewater treatment.

Numerous investigations have been conducted by using various bioadsorbents in the view to remove Congo red from industrial wastewater [14]. Parvin et al. reported considerably high adsorption capacity of chemically treated eggshell membrane (117.65 $mg{\cdot}g^{-1}$) for Congo red removal through adsorption [15]. Rejected tea and tea dust, on the other hand, were reported to be effective adsorbents in case of methylene blue (MB) dye removal with high adsorption capacity of 242.11 $mg{\cdot}g^{-1}$ and 175.4 $mg{\cdot}g^{-1}$, respectively [16,17]. Ghanizadeh and Asgari conducted an experiment for the quest of MB removal by using cattle and sheep bone charcoal as adsorbent where a maximum sorption capacity was found to be 5 $mg{\cdot}g^{-1}$ [18]. Furthermore, a different study was conducted for the removal of methylene blue dye from the wastewater using NaOH modified fish bone charcoal as adsorbent where the extent of sorption capacity was reported to be 605.82 ± 9.09 $mg{\cdot}g^{-1}$ [19]. Although different bioadsorbents were reported to be used in wastewater treatment, bone of silver carp fish, in particular, as an adsorbent in Congo red removal from simulated effluent has not been reported to the best of our knowledge. Silver carp is a very common and locally available fish in Bangladesh. Although different income groups of the country have different levels of fish consumptions, more than 50% of consumption of fish belongs to carp species that includes silver carp with few other species [20]. Huge consumption of silver carp fish generates a considerable number of bones as environmental waste. So, the conversion of this waste to potential adsorbent for dye removal from aqueous solution would be a promising technique to keep environment clean [21].

The aim of this research was to develop an adsorbent from bone of silver carp fish (*Hypophthalmichthys molitrix*) through some simple steps and to find out the potentiality of this adsorbent in removing Congo red from synthetic aqueous solution. In this regard, the influence of several essential operating parameters (e.g., solution pH, dosages of adsorbent, initial concentration of adsorbate, and contact time) on Congo red removal using fish bone powder (FBP) adsorbent was investigated. In addition, adsorption kinetics and equilibrium were analyzed by applying mathematical models to elucidate a plausible adsorption mechanism.

2. Materials and Methods

2.1. Adsorbent Preparation. The fish bone of silver carp (*Hypophthalmichthys molitrix)* was collected from a local fish market (Jashore, Bangladesh). The bones were separated from the fish meat, and the separated fish bones were washed with hot distilled water (343 K) for quite a few times. After that, the washed fish bones were dried under 423 K for 40 min using a drier (DGH-9030) and then cooled down to room temperature. The dried bones were pulverized by using a locally fabricated ball mill, and a particle size of 60 to 100 mesh was taken. The powdered form of fish bone was kept in an airtight container for conducting adsorption studies [19].

2.2. Adsorbate. Congo red (chemical formula: $C_{32}H_{22}N_6Na_2O_6S_2$; molar mass: 696.664 $g{\cdot}mol^{-1}$; $\lambda_{max} = 500$ nm), an anionic dye, was used in this study as an adsorbate. As-received analytical grade Congo red (Merck, Germany) was used in this study. A synthetic stock solution of 1000 $mg{\cdot}L^{-1}$ was prepared by dissolving a required amount of Congo red into a certain amount of distilled water. Varying concentration of Congo red dye solution was prepared by diluting synthetic stock solution of Congo red with distilled water.

2.3. Sample Characterization. Solution pH was measured over the range of 2–8 by a pH meter. Concentrations of dye were measured by a double beam ultraviolet-visible (UV-VIS) spectrophotometer (SHIMADZU UV-1800) at its characteristic wavelength. The functional group of FBP before and after adsorption experiment were determined from infrared (IR) spectra, which were recorded by Perkin Elmer (Spectrum 100) Fourier Transform Infrared (FTIR) spectrophotometer, with a wavelength range of 4,000 cm^{-1} to 400 cm^{-1}.

2.4. Batch Adsorption Study. Batchwise adsorption experiments were conducted to investigate the influence of different parameters, that is, pH (2 to 8), adsorbent dosage (100 mg to 700 mg), contact time (0 to 240 min), and initial dye concentration (50~300 $mg{\cdot}L^{-1}$) on the adsorptive removal of CR. At a certain concentration, measured amount of Congo red solution (100 mL) was taken with a specific amount of FBP in a 250 mL Erlenmeyer flask. The initial pH of each solution was properly adjusted by adding either 0.1 M hydrochloric acid (HCl) or 0.1 M sodium hydroxide (NaOH). Proper mixing of the solutions was done by using a continuous stirrer with a constant speed of 150 rpm and at 303 K for each experiment (unless otherwise stated). After a certain time of stirring, the samples were taken out of the shaker and then filtered. The filtrates were taken for their absorbance measurement. However, removal percentage (% R) of CR dye and the equilibrium amount of dye adsorption ($mg{\cdot}g^{-1}$) was determined by utilizing the following equations [21]:

$$\%R = \frac{C_0 - C_e}{C_0} \times 100, \quad (1)$$

$$q_e = \frac{C_0 - C_e}{w} \times v, \quad (2)$$

where the symbols C_0 and C_e are defined as the initial and final concentration of the Congo red solution ($mg{\cdot}L^{-1}$), respectively, q_e is denoted as the amount of Congo red adsorbed ($mg{\cdot}g^{-1}$), w is symbolized as the weight of FBP adsorbent, and v is termed as the solution quantity in liter (L).

2.5. Kinetics Study. To analyze the CR adsorption mechanism onto FBP, the adsorption kinetics were investigated by using both Lagergren's pseudo-first-order equation (equation (3)) and pseudo-second-order rate equation (equation (4)). The equations can be expressed as follows [21]:

$$\ln(q_e - q_t) = \ln q_e - k_1 t, \quad (3)$$

$$\frac{t}{q_t} = \frac{1}{k_2 q_e^2} + \frac{t}{q_e}, \quad (4)$$

where q_e and q_t are symbolized as the adsorption capacity ($mg{\cdot}g^{-1}$) at equilibrium and that at time t (min), respectively, while k_1 (min^{-1}) and k_2 ($g{\cdot}mg^{-1}{\cdot}min^{-1}$) are termed as the reaction rate constant for Lagergren's pseudo-first-order model and pseudo-second-order model, respectively.

In order to examine the inherent mechanism of the Congo red adsorption onto FBP, the intraparticle diffusion model, as well as Bangham's equation, was also investigated. Intraparticle diffusion can be well explained according to Weber–Morris model, which is expressed as follows [22]:

$$q_t = k_{i\,d} t^{(1/2)} + I, \quad (5)$$

where q_t is denoted as the amount of CR dye adsorbed per an unit mass of FBP adsorbent ($mg{\cdot}g^{-1}$) at time t and k_{id} is termed as the rate constant for intraparticle diffusion model ($mg{\cdot}g^{-1}{\cdot}min^{-1/2}$).

On the other hand, Bangham's pore diffusion model can be equated as follows [23,24]:

$$\log\left[\log\left(\frac{C_0}{C_0 - q_t \cdot m}\right)\right] = \log\left(\frac{k_0 \cdot m}{2.303 \cdot v}\right) + \sigma \cdot \log t, \quad (6)$$

where m ($g{\cdot}L^{-1}$) is adsorbent concentration and k_0 and σ are constants (often called Bangham's parameters), while C_0, q_t, and v possess their usual meaning as stated earlier in this article.

2.6. Isotherm Study. To explain the equilibrium distribution of dye particles onto the surfaces of FBP, the three most common adsorption isotherm models were studied. In this study, the Langmuir isotherm, the Freundlich isotherm, and the Temkin isotherm models were analyzed, which were mentioned correspondingly in the following equations [25]:

$$\frac{C_e}{q_e} = \frac{1}{bq_m} + \frac{C_e}{q_m}, \quad (7)$$

$$\log q_e = \log k_F + \frac{1}{n} \log C_e, \quad (8)$$

$$q_e = BlnK_T + BlnC_e, \quad (9)$$

where C_e ($mg{\cdot}L^{-1}$) signifies the equilibrium adsorbate (CR) concentration, while q_e ($mg{\cdot}g^{-1}$) and q_m ($mg{\cdot}g^{-1}$) indicate the equilibrium sorption capacity and the maximum capacity of sorption of the adsorbent, respectively, b ($L{\cdot}mg^{-1}$) indicates the Langmuir adsorption constant related to free energy of adsorption, k_F ($mg{\cdot}g^{-1}$) designates the adsorption capacity at unit concentration, $1/n$ denotes the adsorption intensity, K_T signifies the Temkin equilibrium binding constant ($L{\cdot}mg^{-1}$) corresponding to the maximum binding energy, and B ($kcal{\cdot}mol^{-1}$) is the heat of adsorption ($B = RT/b$).

2.7. Thermodynamic Study. Thermodynamic investigations for adsorption of CR on FBP were conducted by considering four dissimilar temperatures (298, 308, 318, and 328 K) where all other key parameters (e.g., solution pH, solution concentration, and adsorbent dose) were kept constant. The thermodynamic parameters, such as Gibbs energy (ΔG, $kJ{\cdot}mol^{-1}$), enthalpy of adsorption (ΔH, $kJ{\cdot}mol^{-1}$), and entropy of adsorption process (ΔS, $kJ{\cdot}mol^{-1}{\cdot}K^{-1}$), at different temperatures for the adsorption of CR onto FBP surface were calculated from the following equations [26]:

$$\Delta G = -RT \ln q, \quad (10)$$

$$\ln q = \frac{\Delta S}{R} - \frac{\Delta H}{RT}, \quad (11)$$

where R ($kJ{\cdot}mol^{-1}{\cdot}K^{-1}$), T (K), and q ($mg{\cdot}g^{-1}$) indicate the ideal gas constant, temperature, and the uptake capacity related to Langmuir constant, respectively.

3. Results and Discussion

3.1. Characterization of the FBP Adsorbent

3.1.1. General Characterization. The bulk density of the fish bone powder was measured to be 0.67 $g{\cdot}cm^{-3}$. The moisture content and the ash content of the adsorbent were found to be 3.1% and 36%, respectively. The pH of the adsorbent was determined by mixing fish bone powder with distilled water, and the value of pH was found as 7.8.

3.1.2. Determination of pH_{pzc}. The pH of the point of zero charge (pH_{pzc}) is an important parameter that gives idea to understanding the surface chemistry of an adsorbent. It is one of the essential physicochemical parameters that indicate the net charge of an adsorbent when it comes in contact with water [27]. It is defined as pH of the solution at which the surface charge of the adsorbent has zero value. The global surface charge of the adsorbent is negative at pH higher than

pH_{pzc} (i.e., $pH > pH_{pzc}$) and positive at pH lower than pH_{pzc} (i.e., $pH < pH_{pzc}$). Published reports revealed that adsorption of cationic dye occurred at $pH > pH_{pzc}$ due to the existence of some functional groups, such as COO^- and OH^-. On the other hand, the adsorption of anionic dye occurred at $pH < pH_{pzc}$ [28]. In this investigation, pH_{pzc} of the fish bone powder was determined to be 7 as shown in Figure 1. This signifies that at $pH < pH_{pzc}$, the adsorbent surface carries positive charge and at $pH > pH_{pzc}$, the negative charge exists on the adsorbent surface.

3.1.3. FTIR Analysis. Adsorbent surface properties play a vital role in the entire adsorption process [1]. Therefore, the Fourier transform infrared (FTIR) spectrum is very important to understand the functional groups available in an adsorbent. Fish bone powder is supposed to consist of different functional groups on its surface. These functional groups may have acidic or alkaline properties. The FTIR spectra of FBP in case of before Congo red adsorption and after Congo red adsorption are presented in Figure S1(Supplemental File 1). The spectrum of FBP before adsorption shows several peaks at different wavelengths, which indicates that various functional groups are present in the adsorbent. The FTIR spectroscopic study showed strong and broad peak at 3478.85 cm^{-1} and 3415.00 cm^{-1} for hydroxyl group (O-H) stretching of alcohol group for intermolecular bonding, while the peak at 3236.10 cm^{-1} is assigned by O-H stretching of carboxylic group [29]. The medium band at 1638.54 cm^{-1} and 1617.81 cm^{-1} commonly appeared due to N-H bending of amine [29]. The band at 1112 cm^{-1} is due to O-H vibration of methanol. The absorption bands at 613.85 cm^{-1} and 470.15 cm^{-1} signify the presence of PO_3^{-4} group on the adsorbent surface. It is obvious from Figure S1 that the absorption bands (after adsorption) at lower range slightly shifted due to adsorption of Congo red. This can be attributed to the fact that the functional groups present in the adsorbent might be involved in complexation with adsorbate.

3.2. Effect of Solution pH. There are several factors that affect adsorption of anionic dyes. Solution pH is one of them because of its impact on both the active sites of the adsorbent and the ionization process of the dye molecule in the solution. The effect of solution pH on the adsorption process of Congo red is shown in Figure 2. The experiments were conducted by pouring 100 mL Congo red (150 $mg{\cdot}L^{-1}$) into 100 mg of fish bone adsorbent. It was seen that pH of the adsorbate provides a noteworthy effect on the adsorption process of CR onto FBP surface. Maximum adsorption (96.3%) was found to occur at pH 2, while the adsorption decreased with further rise in pH. The Congo red removal decreased from 96.3% to 17% when the pH was changed from 2 to 8. This phenomenon can be explained by different interactions between adsorbate and adsorbent surface, such as electrostatic force, degree of ionization, hydrogen bonding, and speciation. The sulfonate moiety of Congo red contains negative sulfonic groups ($-SO_3^-$), which dissociates to polar groups ($R - SO_3^-$) at acidic medium [30]. Hence, the

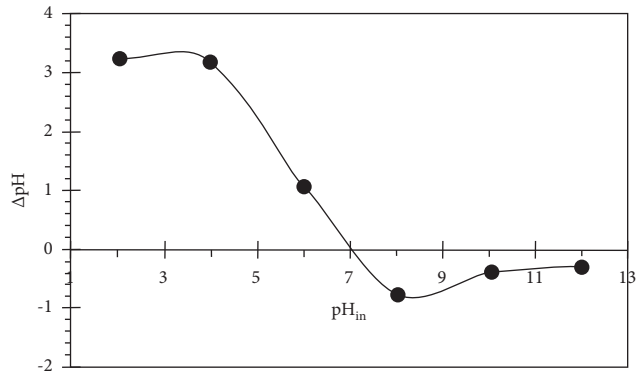

Figure 1: Plot of determination of point of zero charge of fish bone.

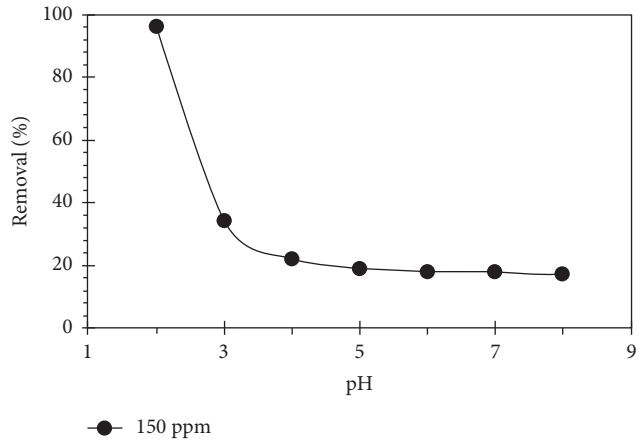

Figure 2: Effect of initial solution pH on Congo red adsorption by fish bone powder (FBP) (adsorbent: 100 mg; adsorbate volume: 100 mL; adsorbate concentration: 150 $mg{\cdot}L^{-1}$; contact time: 4.0 h).

acidic medium favors the adsorption of Congo red onto FBP surface. According to the point of zero charge ($pH_{pzc} = 7$) of fish bone powder shown in Figure 1, the predominant functional groups of the adsorbent surface are positive at $pH < pH_{pzc}$ and negative at $pH > pH_{pzc}$. In acidic condition, the hydrophilic adsorption (electrostatic forces as well as hydrogen bonding) become dominant in the adsorption mechanism. However, the decrease in Congo red removal at higher pH may be due to the competition between excess OH^- ions and dye anions for the adsorption sites. Similar results have been reported for Congo red adsorption on pine bark and activated carbon [11,30]. However, for carrying out further studies using different parameters, the pH value 2 was considered as an optimum value.

3.3. Effect of Adsorbent Dosage on CR Dye Adsorption. The optimum adsorbent dosage is a significant parameter that affects the amount of adsorbed CR by fish bone powder. Varying amounts of FBP (from 100 mg to 700 mg) were used in the present study keeping all other parameters constant. Percent removal of CR is depicted in Figure 3 from where it is obvious that, irrespective of the initial concentrations, removal of Congo red increased from about 91% to 97% with

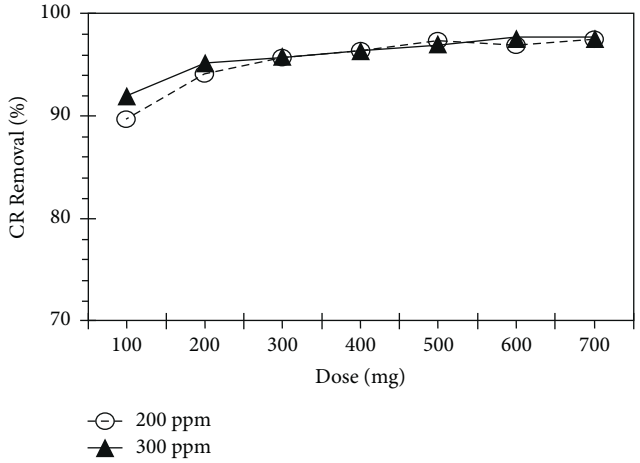

Figure 3: Effect of adsorbent dosages on adsorptive removal of Congo red by using fish bone powder (FBP) (adsorbate volume: 100 mL, pH: 2; adsorbate concentration: 200, 300 mg·L^{-1}; contact time: 4.0 h).

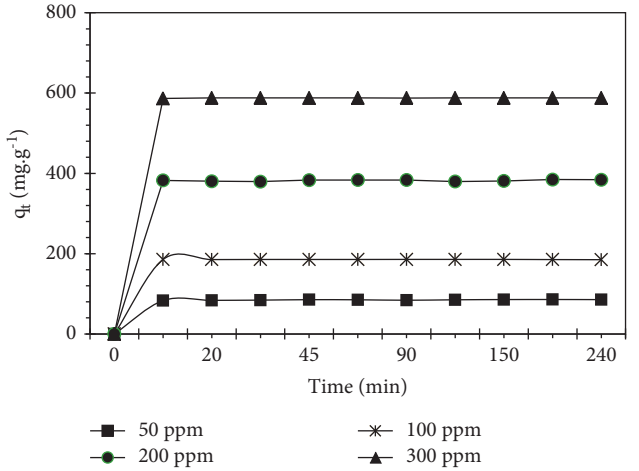

Figure 4: Influence of contact time at various initial concentration on CR removal by fish bone powder (FBP) (adsorbate: 100 mL; pH: 2; adsorbent dose: 500 mg; adsorbate concentration: 50–300 mg·L^{-1}).

increasing adsorbent dosages at the given condition. With the increase in the amount of adsorbent, the total number of active sites of the FBP increases. Therefore, significantly large amount of CR dye can be adsorbed by the FBP resulting in higher dye removal efficiency. Similar results were reported to occur for the Congo red removal by utilizing eggshell membrane [15].

3.4. Effect of Contact Time for Adsorption Reaction at Varying Dye Concentration. In adsorption process, contact time is supposed to be an important parameter to consider because it gives an idea about how long it will take to reach equilibrium. To demonstrate the effect of contact time on adsorption, a series of experiments were conducted by varying the initial concentration of Congo red (50–300 mg·L^{-1}) keeping all other parameters constant. The obtained results are depicted in Figure 4, which demonstrates that the dye uptake (mg·g^{-1}) was very fast at the initial stage (e.g., up to 45 min) after which it became slow and formed plateau. However, for the sake of ensuring a complete reaction, 60 min was selected for performing all other experiments. It is also obtained from Figure 4 that the adsorbed amount of dye increased with the increase in initial concentration. It signifies that the more adsorption sites of the adsorbent were occupied with the increased amount of Congo red. The result is consistent with the findings reported by other research groups [17, 31].

3.5. Adsorption Kinetics. For determining the adsorptive removal mechanism of CR onto FBP surface, two types of kinetic models were studied to analyze the experimental data. The models were (i) pseudo-first-order and (ii) pseudo-second-order kinetic models. Considering the extent of the correlation coefficient (R^2), it was obvious that the process of adsorption could not be well matched by the pseudo-first-order kinetic model. On the other hand, pseudo-second-order kinetic model ((t/q_t)versus t according to (4) was analyzed at different initial CR concentrations, which is shown in Figure 5. It was found that the experimental data fitted very well with pseudo-second-order kinetic model. However, the values of reaction rate constant (k_2), equilibrium uptake capacity (q_e), and correlation coefficient (R^2) were tabulated in Table 1 along with other parameters determined from different models. The values of correlation coefficient were between 0.9999 and 1, while the values of sorption capacities determined from this model ($q_{e,\mathrm{cal}}$) were closer to that obtained experimentally ($q_{e,\mathrm{exp}}$). These outcomes articulate that the pseudo-second-order model can describe the sorption kinetics very well. Similar results were reported for the adsorptive removal of Congo red on various adsorbents, such as pine cone [32], Bengal Gram Seed Husk [33], and eggshell membrane [15].

To reconfirm the best fit kinetic model, the data was further analyzed by squared sum of errors (SSE) method. It is presumed that the lower the value of SSE, the more fit the model. The SSE values for different concentrations were calculated by using the following equation [34]:

$$\mathrm{SSE} = \sum \frac{\left(q_{e,\ \mathrm{exp}} - q_{e,\mathrm{cal}}\right)^2}{q_{e,\ \mathrm{exp}}}, \tag{12}$$

where $q_{e,\mathrm{exp}}$ (mg·L^{-1}) is the experimental sorption capacity at equilibrium and $q_{e,\mathrm{cal}}$ (mg·L^{-1}) is the calculated sorption capacity obtained from corresponding kinetic model. The SSE values for different initial concentrations obtained were tabulated in Table 1. The lower SSE values for pseudo-second-order kinetic model indicated that the sorption kinetics of Congo red onto fish bone powder could be better described by pseudo-second-order model.

3.6. Mass Transfer Mechanism. There are several steps involved in the solid-liquid sorption process. The transmission of the adsorbate initially occurs from the bulk solution to the exterior of the adsorbent. Then, the adsorbate diffuses

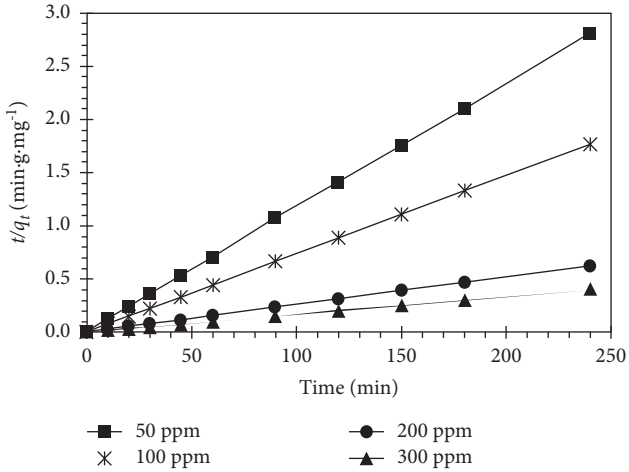

Figure 5: Pseudo-second-order kinetic study.

Table 1: Kinetic parameters for the adsorption of CR onto FBP surface.

C_{in} (mg·L^{-1})	Pseudo-second-order model					Intraparticle diffusion model		Bangham's model		
	$q_{e.cal}$ (mg·g^{-1})	$q_{e.exp}$ (mg·g^{-1})	k_2 (mg·g^{-1}·min^{-1})	R^2	SSE	k_{id2} (mg·g^{-1}·min$^{-1/2}$)	I	k_0	σ	R^2
50	85.47	82.43	0.0253	0.9999	0.1490	4.04	52.82	0.3994	0.0314	0.9644
100	185.13	181.02	0.0456	1	0.0091	8.41	118.10	0.4562	0.0411	0.8565
200	384.61	383.42	0.0112	1	0.2369	17.56	242.09	0.4895	0.0419	0.7802
300	588.23	583.71	0.3612	1	0.0061	26.76	373.75	0.5671	0.0116	0.7588

through the boundary layer and at the end it moves through the pores of the adsorbent. In the course of the transmission of adsorbate, it is adsorbed at the available active sites. Although the pseudo-second-order kinetic model was found to be the best fit model, it did not provide any information regarding mass transfer mechanism. In this study, the mass transfer mechanism was analyzed by using a well-known diffusion model, namely, Weber–Morris intraparticle diffusion model [35]. Diffusion control is supposed to be the most consistent explanation for almost all reported results in which the rate equation of pseudo-second order for adsorption has been found to fit the data well [36]. Intraparticle diffusion model was studied by plotting q_t versus $t^{0.5}$ according to equation (5) and is depicted in Figure 6 where two distinct linear regions are noticed. The first linear region signifies the rapid external surface loading or film diffusion, while the second linear region represents the pore diffusion. The rate constant of pore diffusion (k_{id2}) was determined from the slope of each line, while intercept of each line represented the boundary layer thickness during adsorption process. A schematic diagram of Congo red transport is presented in Figure 7. The calculated values of k_{id} and I are tabulated in Table 1. Similar outcomes were reported for activated carbon as well [37].

The kinetic data for Congo red adsorption on FBP was further interpreted by using Bangham's diffusion model (equation (6)) in order to examine whether or not the pore diffusion was the only rate controlling step in the sorption process. For determining Bangham's parameters, a plot of $\log[\log(C_0/(C_0 - q_t \cdot m))]$ versus $\log t$ for different initial concentration was drawn as shown in Figure S2 (Supplemental File 2). The plot was found to be linear for each initial concentration. Bangham's parameters (k_0 and σ) were calculated from the intercept and slope, respectively, and were tabulated in Table 1. The correlation coefficients for different initial concentrations were in a range from 0.9644 to 0.7588. According to the above-mentioned analysis, it could be concluded that both film diffusion and pore diffusion are involved in different stages of the sorption process [24].

3.7. Adsorption Isotherm Studies. Isotherms of adsorption are the indicative of adsorbate partitioning among the solid phase (adsorbent) as well as the liquid phase (adsorbate). The isotherms find the extent of adsorption of certain adsorbate onto a specific adsorbent at defined conditions. In this present study, two common isotherm models were used to discuss the adsorption isotherms for CR removal onto FBP at pH 2. The discussed models were Langmuir as well as Freundlich isotherm models by which the data were analyzed.

Langmuir isotherm model considers a monolayer adsorption process where the sorption occurs at homogeneous surfaces of the adsorbent. In this case, by using equation (7), $(1/q_e)$ versus $(1/C_e)$ is plotted, which is shown in Figure 8(a). The maximum sorption capacity q_m (mg·g^{-1}) and the Langmuir constant b (L·mg^{-1}) are determined from the slope and intercept of the straight line, respectively.

Freundlich isotherm model (equation (8)), on the other hand, is supposed to be applied for adsorption of adsorbent on heterogeneous surfaces. This model can deal with

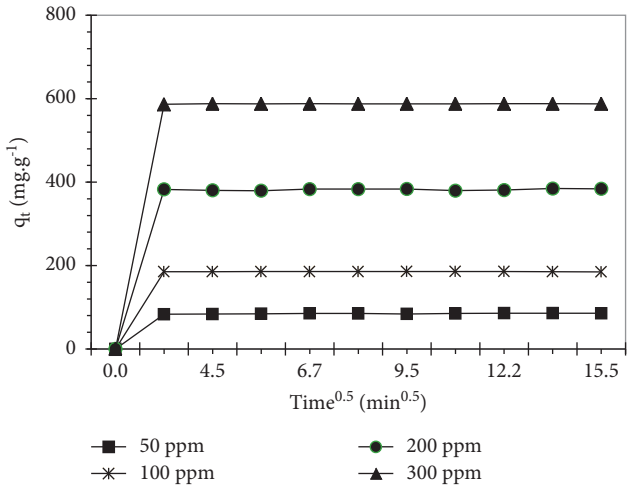

Figure 6: Intraparticle diffusion analysis.

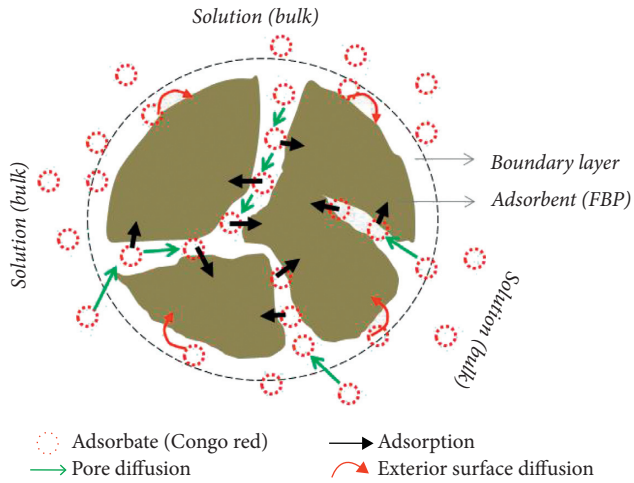

Figure 7: Schematic diagram of Congo red transport and sorption mechanism.

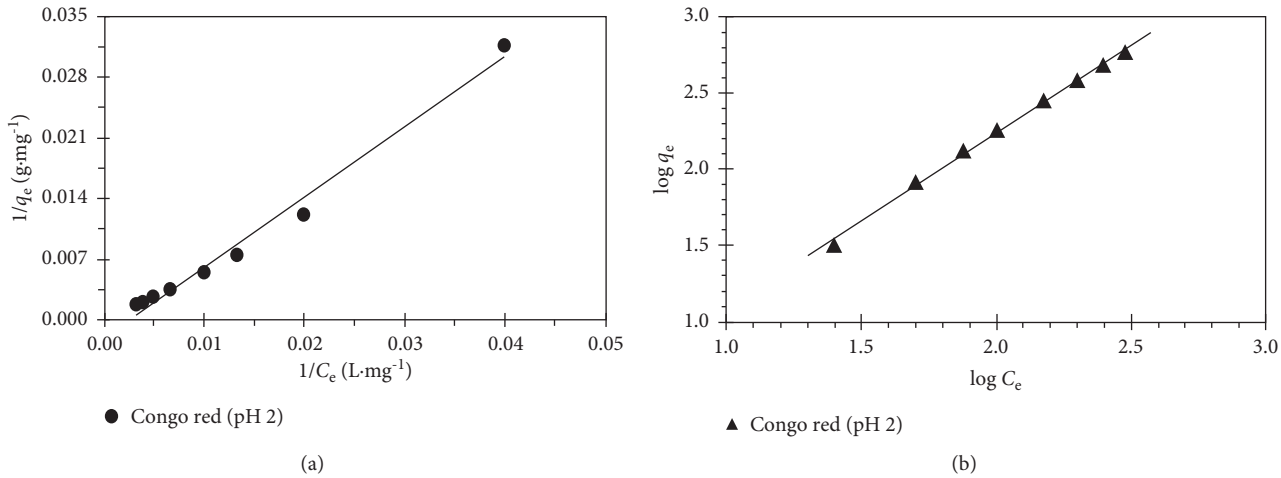

Figure 8: Isotherm analysis using (a) Langmuir and (b) Freundlich model.

multilayer adsorption process too. However, the related parameters such as K_F and n can be determined from the intercept and slope of the straight line of a plot log C_e versus log q_e, which is depicted in Figure 8(b). Temkin isotherm parameters such as Temkin isotherm constant (K_T) and heat of adsorption (B) are determined from the slope and intercept of the plot of a plot q_e versus ln C_e (for simplicity figure not shown) by using equation (9).

The extent of different isotherm parameters obtained from the above-mentioned analyses is tabulated in Table 2. On the basis of the extent of the correlation coefficients, it can be summarized that the adsorption process can be better explained by using the Langmuir isotherm model ($R^2 = 0.9929$) compared to the Freundlich and Temkin isotherm models. Thus, the result indicated that a monolayer adsorption occurred during the discussed adsorption process. Similar findings were reported by various researchers for different adsorbents [15, 33, 38]. It is noteworthy to mention that the adsorption capacity of the current adsorbent (FBP) is considerably high compared to other biomaterial-derived adsorbents as shown in Table 3.

3.8. Effect of Temperature and Thermodynamic Studies. The effect of temperature on Congo red adsorption from aqueous solution using fish bone powder was tested in this study. Batch experiments were carried out at varying temperatures keeping all other parameters constant. The results are depicted in Figure 9 where it is evident that the removal of Congo red increases from 141 mg·g^{-1} to 381 mg·g^{-1} with the increase in temperature from 298 K to 328 K. An increase in temperature leads to fast diffusion of Congo red molecules through the external boundary layer and the internal pores of the adsorbent due to less resistance offered by viscous forces in the aqueous phase [41]. Moreover, the increase in sorption capacity at elevated temperature may happen due to the pore size enlargement of the adsorbent [42].

Thermodynamic parameters are the essential parametric tools to understand whether the adsorption process is physical or chemical, spontaneous or nonspontaneous, and exothermic or endothermic. To determine these parameters, ln q versus $(1/T)$ was plotted using equation (11), which is shown in Figure 10. The values of change in enthalpy (ΔH) and entropy (ΔS) can be determined from the slope and intercept of the graphical plot, while the values of Gibbs energy (ΔG) are calculated by using equation (10). However, the thermodynamic parameters calculated from this study are presented in Table 4. From the table, it is obvious that the values of ΔG become successively more negative with the temperature rise. Such phenomenon signifies the process of CR adsorption onto FBP surface is spontaneous and feasible. The positive value of change in enthalpy indicates that the adsorption is endothermic in nature, which can be substantiated by the increase in adsorption capacity with increase in temperature. To know about the binding method between Congo red and fish bone powder, the activation energy (Ea) of the adsorption process was determined as well. Physical adsorption (physisorption) generally has low activation energy (<40 kJ·mol^{-1}), while chemical adsorption (chemisorption) has considerably high activation energy (>40 kJ·mol^{-1}) [43]. The activation energy was determined to be 29.84 kJ·mol^{-1}, which indicated that the adsorption process was of physisorption type. On the other hand, the affinity and increased randomness or disorderliness at the adsorbent-adsorbate interface during the period of adsorption of Congo red by FBP were corroborated by the positive value of ΔS [15,44].

Table 2: Linearized isotherm coefficients for Congo red adsorption onto FBP surface.

Isotherms	Parameters	Value
Langmuir isotherm	q_m (mg·g^{-1})	666.67
	b (L·mg^{-1})	0.0020
	R^2	0.9929
Freundlich isotherm	K_F (L·mg^{-1})	1.358
	N	0.848
	R^2	0.9895
Temkin isotherm	B (kcal·mol^{-1})	0.05
	K_T (L·mg^{-1})	0.031
	R^2	0.8971

Table 3: Comparison of sorption capacities of low-cost adsorbents for various dyes.

Materials	Dye	q_m (mg·g^{-1})	References
Fish bone powder (FBP)	CR	666.67	In this work
Fish bone	BB41, BY28	37.36	[4]
Eggshell membrane	CR	117.65	[15]
Modified fishbone charcoal	MB	605.82	[19]
Untreated fishbone charcoal	MB	70.42	[19]
Raw pine cone	CR	32.65	[32]
Acid-treated pine cone	CR	40.19	[32]
Bone char	AR.TF	73.91	[39]
Tuna fish bone	CR	329.0	[40]

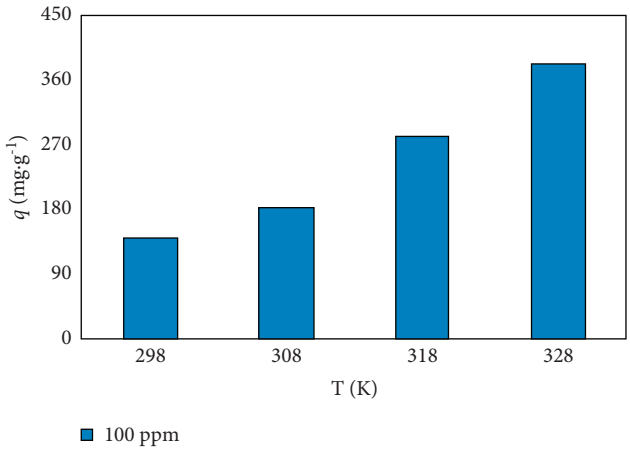

Figure 9: Effect of temperature on Congo red removal by fish bone powder.

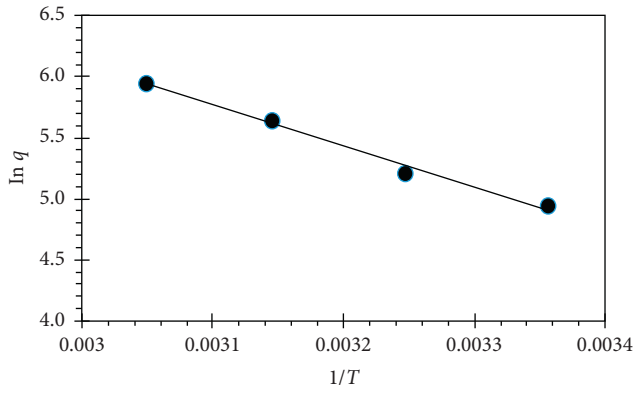

Figure 10: Thermodynamic study of adsorption of Congo red on fish bone powder.

Table 4: Thermodynamic parameters for the adsorption of Congo red on FBP.

T (K)	ΔG (kJ·mol^{-1})	ΔH (kJ·mol^{-1})	ΔS (kJ·mol^{-1}·K^{-1})
298	−12.26	27.70	0.13
308	−13.34		
318	−14.91		
328	−16.19		

4. Conclusion

This research investigated the applicability of fish bone as an adsorbent in the view to the anionic dye (Congo red) removal from synthetic wastewater solution. The isoelectric point (pH_{PZC}) indicated that the adsorbent surface is positive below the value of pH 7, which resulted in a favorable Congo red adsorption at low pH. From the analysis of kinetic data, it was obvious that the adsorption of Congo red followed a pseudo-second-order reaction model. Experimental data was analyzed with different models of isotherm, and it was perceived that the Langmuir isotherm model fitted very well with the experimentally obtained data compared with Freundlich and Temkim isotherm models. The maximum sorption capacity was evaluated to be 666.67 mg·g^{-1}. The extent of activation energy (29.84 kJ·mol^{-1}) confirmed that the binding between Congo red and fish bone powder occurred through a physisorption process. In addition to this, the adsorption process was observed to be endothermic and spontaneous in nature. The findings of this research proclaimed that fish bone powder derived from a locally available fish (silver carp) can be an effective adsorbent for Congo red removal from wastewater.

Data Availability

The data used to support the findings of this study are available from the corresponding author upon request.

Conflicts of Interest

The authors declare that they have no known conflicts of interest or personal relationships that could have appeared to influence the work reported in this paper.

Authors' Contributions

Shahanaz Parvin was responsible for conceptualization, methodology, validation, and supervision. Manjur Hussain and Farhana Akter were responsible for investigation, formal analysis, and writing of the original draft. Biplob Kumar Biswas was responsible for conceptualization, supervision, and review and editing of the manuscript.

Supplementary Materials

Figure S1: FTIR spectra of the fish bone powder (a) before and (b) after adsorption. Figure S2: Bangham's diffusion model for Congo red adsorption by fish bone powder adsorbent. (*Supplementary Materials*)

References

[1] R. Ahmad and R. Kumar, "Adsorptive removal of congo red dye from aqueous solution using bael shell carbon," *Applied Surface Science*, vol. 257, no. 5, pp. 1628–1633, 2010.

[2] N. Dizge, C. Aydiner, E. Demirbas, M. Kobya, and S. Kara, "Adsorption of reactive dyes from aqueous solutions by fly ash: kinetic and equilibrium studies," *Journal of Hazardous Materials*, vol. 150, no. 3, pp. 737–746, 2008.

[3] M. J. Iqbal and M. N. Ashiq, "Adsorption of dyes from aqueous solutions on activated charcoal," *Journal of Hazardous Materials*, vol. 139, no. 1, pp. 57–66, 2007.

[4] A. Ebrahimi, M. Arami, H. Bahrami, and E. Pajootan, "Fish bone as a low-cost adsorbent for dye removal from wastewater: response surface methodology and classical method," *Environmental Modeling & Assessment*, vol. 18, no. 6, pp. 661–670, 2013.

[5] M. T. Yagub, T. K. Sen, S. Afroze, and H. M. Ang, "Dye and its removal from aqueous solution by adsorption: a review," *Advances in Colloid and Interface Science*, vol. 209, pp. 172–184, 2014.

[6] M. A. H. Dhaif-Allah, S. N. Taqui, U. T. Syed, and A. A. Syed, "Kinetic and isotherm modeling for acid blue 113 dye adsorption onto low-cost nutraceutical industrial fenugreek seed spent," *Applied Water Science*, vol. 10, no. 2, 2020.

[7] R. K. Prasad, "Color removal from distillery spent wash through coagulation using *Moringa oleifera* seeds: use of optimum response surface methodology," *Journal of Hazardous Materials*, vol. 165, no. 1-3, pp. 804–811, 2009.

[8] N. P. Khumalo, G. D. Vilakati, S. D. Mhlanga et al., "Dual-functional ultrafiltration nano-enabled PSf/PVA membrane for the removal of Congo red dye," *Journal of Water Process Engineering*, vol. 31, Article ID 100878, 2019.

[9] M. Panizza, A. Barbucci, R. Ricotti, and G. Cerisola, "Electrochemical degradation of methylene blue," *Separation and Purification Technology*, vol. 54, no. 3, pp. 382–387, 2007.

[10] E. G. Solozhenko, N. M. Soboleva, and V. V. Goncharuk, "Decolourization of azodye solutions by Fenton's oxidation," *Water Research*, vol. 29, no. 9, pp. 2206–2210, 1995.

[11] K. Litefti, M. S. Freire, M. Stitou, and J. González-Álvarez, "Adsorption of an anionic dye (congo red) from aqueous solutions by pine bark," *Scientific Reports*, vol. 9, no. 1, p. 16530, 2019.

[12] F. Kallel, F. Chaari, F. Bouaziz, F. Bettaieb, R. Ghorbel, and S. E. Chaabouni, "Sorption and desorption characteristics for the removal of a toxic dye, methylene blue from aqueous

solution by a low cost agricultural by-product," *Journal of Molecular Liquids*, vol. 219, pp. 279–288, 2016.

[13] R. Slimani, A. Anouzla, Y. Abrouki et al., "Removal of a cationic dye-Methylene Blue-from aqueous media by the use of animal bone meal as a new low cost adsorbent," *Journal of Materials and Environmental Science*, vol. 2, no. 1, pp. 77–87, 2011.

[14] P. Bhatia and M. Nath, "Green synthesis of p-NiO/n-ZnO nanocomposites: excellent adsorbent for removal of Congo red and efficient catalyst for reduction of 4-nitrophenol present in wastewater," *Journal of Water Process Engineering*, vol. 33, Article ID 101017, 2020.

[15] S. Parvin, B. K. Biswas, M. A. Rahman, M. H. Rahman, M. S. Anik, and M. R. Uddin, "Study on adsorption of congo red onto chemically modified egg shell membrane," *Chemosphere*, vol. 236, Article ID 124326, 2019.

[16] N. Nasuha and B. H. Hameed, "Adsorption of methylene blue from aqueous solution onto NaOH-modified rejected tea," *Chemical engineering journal*, vol. 166, no. 2, pp. 783–786, 2011.

[17] M. M. R. Khan, M. W. Rahman, H. R. Ong, A. B. Ismail, and C. K. Cheng, "Tea dust as a potential low-cost adsorbent for the removal of crystal violet from aqueous solution," *Desalination and Water Treatment*, vol. 57, no. 31, pp. 14728–14738, 2016.

[18] G. Ghanizadeh and G. Asgari, "Adsorption kinetics and isotherm of methylene blue and its removal from aqueous solution using bone charcoal," *Reaction Kinetics, Mechanisms and Catalysis*, vol. 102, no. 1, pp. 127–142, 2011.

[19] W. Wang, Y.-Y. Liu, X.-F. Chen, and S.-X. Song, "Facile synthesis of NaOH-modified fishbone charcoal (FBC) with remarkable adsorption towards methylene blue," *Procedia engineering*, vol. 211, pp. 495–505, 2018.

[20] M. F. Alam, "Socioeconomic aspects of carp production and consumption in Bangladesh," in *Proceedings of a Workshop on Genetic Management and Improvement Strategies for Exotic Carps in Asia*, Dhaka, Bangladesh, February 2002.

[21] J. M. Jabar, Y. A. Odusote, K. A. Alabi, and I. B. Ahmed, "Kinetics and mechanisms of congo-red dye removal from aqueous solution using activated *Moringa oleifera* seed coat as adsorbent," *Applied Water Science*, vol. 10, no. 6, p. 136, 2020.

[22] W. J. Weber Jr and J. C. Morris, "Kinetics of adsorption on carbon from solution," *Journal of the Sanitary Engineering Division*, vol. 89, no. 2, pp. 31–59, 1963.

[23] A. Pholosi, E. B. Naidoo, and A. E. Ofomaja, "Intraparticle diffusion of Cr(VI) through biomass and magnetite coated biomass: a comparative kinetic and diffusion study," *South African Journal of Chemical Engineering*, vol. 32, no. 1, pp. 39–55, 2020.

[24] U. A. Edet and A. O. Ifelebuegu, "Kinetics, isotherms, and thermodynamic modeling of the adsorption of phosphates from model wastewater using recycled brick waste," *Processes*, vol. 8, no. 6, p. 665, 2020.

[25] S. Kumari, D. Mankotia, and G. S. Chauhan, "Crosslinked cellulose dialdehyde for Congo red removal from its aqueous solutions," *Journal of environmental chemical engineering*, vol. 4, no. 1, pp. 1126–1136, 2016.

[26] M. E. Argun, S. Dursun, C. Ozdemir, and M. Karatas, "Heavy metal adsorption by modified oak sawdust: thermodynamics and kinetics," *Journal of Hazardous Materials*, vol. 141, no. 1, pp. 77–85, 2007.

[27] V. Bernal, L. Giraldo, and J. Moreno-Piraján, "Physicochemical properties of activated carbon: their effect on the adsorption of pharmaceutical compounds and adsorbate-adsorbent interactions," *Chimia*, vol. 4, no. 4, p. 62, 2018.

[28] D. Savova, N. Petrov, M. F. Yardim et al., "The influence of the texture and surface properties of carbon adsorbents obtained from biomass products on the adsorption of manganese ions from aqueous solution," *Carbon*, vol. 41, no. 10, pp. 1897–1903, 2003.

[29] Website of Sigma-Aldrich, "IR spectrum table and chart," 2021, https://www.sigmaaldrich.com/technical-documents/articles/biology/ir-spectrum-table.html.

[30] R. Lafi, I. Montasser, and A. Hafiane, "Adsorption of congo red dye from aqueous solutions by prepared activated carbon with oxygen-containing functional groups and its regeneration," *Adsorption Science & Technology*, vol. 37, no. 1-2, pp. 160–181, 2019.

[31] M. Dehvari, M. H. Ehrampoush, M. T. Ghaneian, B. Jamshidi, and M. Tabatabaee, "Adsorption kinetics and equilibrium studies of reactive red 198 dye by cuttle powder," *Iranian Journal of Chemistry & Chemical Engineering-International English Edition*, vol. 36, no. 2, pp. 143–151, 2017.

[32] S. Dawood and T. K. Sen, "Removal of anionic dye congo red from aqueous solution by raw pine and acid-treated pine cone powder as adsorbent: equilibrium, thermodynamic, kinetics, mechanism and process design," *Water Research*, vol. 46, no. 6, pp. 1933–1946, 2012.

[33] M. C. Somasekhara Reddy, V. Nirmala, and C. Ashwini, "Bengal gram seed husk as an adsorbent for the removal of dye from aqueous solutions-batch studies," *Arabian Journal of Chemistry*, vol. 10, no. 2, pp. S2554–S2566, 2017.

[34] C. Chakrapani, C. S. Babu, K. N. K. Vani, and S. Rao, "Adsorption kinetics for the removal of fluoride from aquesou solution by activated carbeon adsorbents derived from the peels of selected citrus fruits," *E-Journal of Chemistry*, vol. 7, no. S1, pp. S419–S427, Article ID 582150, 2010.

[35] B. H. Hameed and M. I. El-Khaiary, "Removal of basic dye from aqueous medium using a novel agricultural waste material: pumpkin seed hull," *Journal of Hazardous Materials*, vol. 155, no. 3, pp. 601–609, 2008.

[36] M. Hubbe, S. Azizian, and S. Douven, "Implications of apparent pseudo-second-order adsorption kinetics onto cellulosic materials: a review," *BioResources*, vol. 14, no. 3, pp. 7582–7626, 2019.

[37] Z. Cheng, L. Zhang, X. Guo, X. Jiang, and T. Li, "Adsorption behavior of direct red 80 and Congo red onto activated carbon/surfactant: process optimization, kinetics and equilibrium," *Spectrochimica Acta Part A: Molecular and Biomolecular Spectroscopy*, vol. 137, pp. 1126–1143, 2015.

[38] A. H. Jawad, R. A. Rashid, R. M. A. Mahmuod, M. A. M. Ishak, N. N. Kasim, and K. Ismail, "Adsorption of methylene blue onto coconut (*Cocos nucifera*) leaf: optimization, isotherm and kinetic studies," *Desalination and Water Treatment*, vol. 57, no. 19, pp. 8839–8853, 2016.

[39] R. A. Moura, A. A. Seolatto, M. E. De Oliveira Ferreira, and F. F. Freitas, "The adsorption study of Royal Blue Tiafix and Black Tiassolan dyes using bone char as adsorbent," *Adsorption Science & Technology*, vol. 36, no. 3-4, pp. 1178–1198, 2018.

[40] Q. Peng, F. Yu, B. Huang, and Y. Huang, "Carbon-containing bone hydroxyapatite obtained from tuna fish bone with high adsorption performance for Congo red," *RSC Advances*, vol. 7, no. 43, pp. 26968–26973, 2017.

[41] S. Banerjee and M. C. Chattopadhyaya, "Adsorption characteristics for the removal of a toxic dye, tartrazine from aqueous solutions by a low cost agricultural by-product," *Arabian Journal of Chemistry*, vol. 10, no. 2, pp. S1629–S1638, 2017.

[42] E. Demirbas, M. Kobya, and M. T. Sulak, "Adsorption kinetics of a basic dye from aqueous solutions onto apricot stone activated carbon," *Bioresource Technology*, vol. 99, no. 13, pp. 5368–5373, 2008.

[43] V. J. Inglezakis and A. A. Zorpas, "Heat of adsorption, adsorption energy and activation energy in adsorption and ion exchange systems," *Desalination and Water Treatment*, vol. 39, pp. 149–157, 2012.

[44] Y. T. Gebreslassie, "Equilibrium, kinetics, and thermodynamic studies of malachite green adsorption onto Fig (*Ficus cartia*) leaves," *Journal of analytical methods in chemistry*, vol. 2020, Article ID 7384675, 11 pages, 2020.